STRUCTURAL INSIGHTS INTO PRE-TRANSLOCATION RIBOSOME MOTIONS

SAMUEL COULBOURN FLORES
Bioengineering Department, Stanford University, James H Clark Center S172 MC:5448
Stanford, California 94305, USA
Email: samuelflorec@gmail.com

RUSS ALTMAN
Bioengineering Department, Stanford University, James H Clark Center S231 MC:5444
Stanford, California 94305, USA
Email: russ.altman@stanford.edu

Subsequent to the peptidyl transfer step of the translation elongation cycle, the initially formed pre-translocation ribosome, which we refer to here as R_1, undergoes a ratchet-like intersubunit rotation in order to sample a rotated conformation, referred to here as R_F, that is an obligatory intermediate in the translocation of tRNAs and mRNA through the ribosome during the translocation step of the translation elongation cycle. R_F and the R_1 to R_F transition are currently the subject of intense research, driven in part by the potential for developing novel antibiotics which trap R_F or confound the R_1 to R_F transition. Currently lacking a 3D atomic structure of the R_F endpoint of the transition, as well as a preliminary conformational trajectory connecting R_1 and R_F, the dynamics of the mechanistically crucial R_1 to R_F transition remain elusive. The current literature reports fitting of only a few ribosomal RNA (rRNA) and ribosomal protein (r-protein) components into cryogenic electron microscopy (cryo-EM) reconstructions of the *Escherichia coli* ribosome in R_F. In this work we now fit the entire *Thermus thermophilus* 16S and 23S rRNAs and most of the remaining *T. thermophilus* r-proteins into a cryo-EM reconstruction of the *E. coli* ribosome in RF in order to build an almost complete model of the *T. thermophilus* ribosome in R_F thus allowing a more detailed view of this crucial conformation. The resulting model validates key predictions from the published literature; in particular it recovers intersubunit bridges known to be maintained throughout the R_1 to R_F transition and results in new intersubunit bridges that are predicted to exist only in R_F. In addition, we use a recently reported *E. coli* ribosome structure, apparently trapped in an intermediate state along the R_1 to R_F transition pathway, referred to here as R_2, as a guide to generate a *T. thermophilus* ribosome in the R_2 state. This demonstrates a multiresolution method for morphing large complexes and provides us with a structural model of R_2 in the species of interest. The generated structural models form the basis for probing the motion of the deacylated tRNA bound at the peptidyl-tRNA binding site (P site) of the pre-translocation ribosome as it moves from its so-called classical P/P configuration to its so-called hybrid P/E configuration as part of the R_1 to R_F transition. We create a dynamic model of this process which provides structural insights into the functional significance of R_2 as well as detailed atomic information to guide the design of further experiments. The results suggest extensibility to other steps of protein synthesis as well as to spatially larger systems.

1. Introduction

The structure of the ribosome is surprisingly well conserved across the kingdoms of life and is thus biologically interesting for what its structure and, potentially, dynamics tell us about evolution. Multiple structures of bacterial (mostly *Escherichia coli* and *Thermus thermophilus*) ribosomes in complex with their tRNA substrates have been solved crystallographically [1], while others have

been solved at low resolution by cryogenic electron microscopy (cryo-EM) [2]. However, the motions connecting these static conformational states of the ribosome and its bound tRNA substrates are currently the subject of intense research. In order to provide initial insight and focus further experiments, it would be useful to have at least a preliminary trajectory of motion connecting all of the states encompassing a cycle of translation, generated initially by flexible alignment or morphing. For this, we must translate all crystallographic structures into a single species, and fit all-atom models into cryo-EM density maps, and then connect the states by flexible alignment. We show how the recently announced RNABuilder modeling code and other tools can be used to accomplish this. We focus on the conformational changes of the ribosome as it undergoes a critical ratchet-like intersubunit rotation and on the associated reconfiguration of the deacylated tRNA bound at the peptidyl-tRNA binding site (P site) of the ribosomal pre-translocation complex from its so-called classical P/P configuration to its so-called hybrid P/E configuration. We model these conformational changes by a flexible alignment to ribosomal structures in three presumably sequential conformational states. The resulting dynamic model highlights important phenomena and provides a structural basis for the design of further experiments.

2. Background

2.1. *Multi-resolution modeling at the mesoscale*

The ribosome, by its sheer size, challenges conventional computational techniques and calls for new approaches. Multi-resolution modeling (MRM) refers to the treatment of different molecules, domains, spatial regions, or time spans in a system at different levels of resolution, either from the force field or kinematic perspective [3]. A wide variety of techniques fall under this paradigm. Some workers, for example, treat lipids and water using a reduced set of pseudoatoms, while modeling a protein inserted in the membrane at full-atomic resolution. Others collect statistics from experiments or short-time Molecular Dynamics (MD) simulations at fine resolution, and use these statistics to parameterize a coarse-grained force field, thus separating the resolutions in time. Still others run a fine and a coarse grained simulation simultaneously for the same system and exchange resolution from time to time, in an approach known as Resolution Exchange [3].

Mesoscale modeling refers to the structural and dynamic study of phenomena at length scales between those of single molecules (which can be modeled with MD and related methods) and those of extended tissues (which may be best modeled using continuum mechanics approaches) [4]. Some examples of this are actin filament elongation, muscle function, chromatin remodeling, and mitosis.

Internal Coordinate Mechanics (ICM) refers to a calculation in which bodies are connected to other bodies using *mobilizers* which may grant zero to six degrees of freedom [5]. In ICM, computer time is only spent computing the degrees of freedom granted by the mobilizers, whereas in MD reducing the degrees of freedom actually *increases* expense by adding constraint equations which must then be solved. The mobilizers connect bodies in a tree structure, and the calculation of position, velocity, and acceleration begins at the base body and proceeds up the tree. In an ICM framework, bodies may consist of one or more atoms, and the connections between atoms may permit dihedral angle changes but leave bond lengths and angles fixed. This characteristic makes ICM an ideal

approach to MRM, because arbitrary domains, molecules, and complexes which are converged or uninteresting may be rigidified for economy and other modeling goals. Note that so far we have only described coarse graining the *kinematics;* the atoms within rigidified regions can still have force interactions with atoms in other regions.

RNABuilder is an ICM, MRM code which allows the user to instantiate molecules, match their structural coordinates to input files, control their flexibility, and apply base pairing, steric, and other atomic interaction forces. The user can further control most simulation parameters, including temperature, run time, output frequency, and type of time integrator and thermostat. A wide variety of applications are possible, such as structure prediction from base pairing contacts [6], refinement, threading [7], and flexible alignment. We have instantiated RNA chains as long as 13000 residues [5]; we have also shown that computer time can have order-N scaling with molecule size. This suggests that the presented methods are applicable to problems that approach the mesoscale.

2.2. *Progress and limitations in ribosome structure*

The past decade has seen an explosion of discoveries in ribosome structure. The state of the pre-translocation ribosomal complex that is sampled immediately following peptidyl transfer, which we refer to here as R_1, following the nomenclature recently introduced by Cate and co-workers[8], is particularly well characterized[9]. The structures of a number of other states have also been solved, if not crystallographically[1] then by cryo-EM [2]. The full story of ribosome function, however, involves the structural dynamics connecting the various observed states. Knowing these details will lead to a more fundamental understanding of protein synthesis across all kingdoms of life and promises to guide the development of novel antibiotics which function by confounding dynamics crucial to function. As a future goal, we wish to generate an all-atom trajectory of the entire translation cycle. For this we face two challenges: first, structures of the various available states have been solved using ribosomes and biomolecular components isolated from a variety of species, mostly *E. coli* and *T. thermophilus,* and second, some of these structures have been solved by cryo-EM and are available only as electron density maps. In this work we show how to address both these issues with the help of RNABuilder and other packages.

2.3. *Structure of the ribosome in the fully rotated R_F conformation*

Immediately following peptidyl transfer, the pre-translocation ribosome, initially in R_1, undergoes a ratchet-like intersubunit rotation in order to sample a rotated conformation, referred to here as R_F, that is an obligatory intermediate in the translocation of tRNAs and mRNA through the ribosome during the translocation step of the translation elongation cycle. Unlike R_1, atomic resolution structures of R_F remain elusive and, although considerable structural insight has come from cryo-EM reconstructions of R_F, these workers typically only published fits of those ribosomal and/or tRNA components and/or fragments of components needed to answer specific structural questions. As a consequence, a published and widely available all-atom model of R_F, based on the fitting of atomic resolution structures to cryo-EM reconstructions of R_F, is not currently available. In this work we report an all-atom model of R_F built by fitting atomic resolution structures to cryo-EM reconstructions of R_F [2]. This provides structural insights not obvious from inspection of the raw density of the reconstruction and promises to be useful for understanding the details of intersubunit interactions in the context of biochemical experiments[10].

2.4. *Structure of the ribosome in the intermediate R_2 state, and the R_1-R_2-R_F trajectory*

A recent structure of the ribosome in complex with P and A site-bound anticodon stem-loops (ASLs) rather than full-length tRNAs reveals a ribosome conformation that is apparently in an intermediate state of intersubunit rotation, referred to here as R_2, that lies somewhere between R_1 and R_F [8]. Interestingly, the ASLs in R_2 are positioned in a way that suggests that full-length tRNAs, should they have been present in the ribosomal complex that was crystallized, would be in their hybrid configurations. Nevertheless, the lack of full-length tRNAs in the ribosomal complex used to solve the R_2 structure and the associated lack of tRNA-ribosome interactions that would ordinarily be made between full-length tRNAs and the ribosome in R_2, leave open the question of how full-length tRNAs would be positioned within R_2. The current work addresses this question by constructing putative trajectories of motion connecting R_1, R_2, and R_F. This gives us a dynamic view of the trajectory of motion from R_1 to R_F, rather than the more typical view gained by inspection of static structures.

3. Method

3.1. *Creating the T.thermophilus R_2 structure by morphing*

As mentioned above, the crystallographically observed R_2 structure is inconvenient for our purposes because it was solved using *E. coli* ribosomes, whereas we are working with *T. thermophilus* ribosomes. We solved this problem by morphing the *T. thermophilus* R_1 structure onto the *E. coli* R_2 structure, thus copying the R_2 conformation onto the *T. thermophilus* ribosome.

To generate this morph we flexibilized the neck region (which connects the head to the body domain) as well as the base of the beak domain on the small ribosomal subunit and the base of the L1 stalk domain of the large ribosomal subunit (see **Figure 1** for a map of ribosomal domains and structural figures). We restrained the P-site tRNA into the classical P/P configuration by enforcing two Watson-Crick base pairs between the aminoacyl acceptor stem of the tRNA and the 23 rRNA nucleotides comprising the so-called P loop within the P site of the peptidyl transferase center and enforcing three Watson-Crick base pairs between the anticodon stem-loop of the tRNA and the mRNA codon. Likewise, we restrained the E-site tRNA into the classical E/E configuration using a base stacking sandwich involving the tRNA 5' terminal residue, and by a Weld constraint to an apparent tRNA-binding domain on ribosomal protein S7 (the tRNA binding domain was connected to the rest of S7 by a flexible hinge). The majority of ribosomal proteins were rigid and fixed to the corresponding domain on the 23S or 16S rRNA. The system also included the 16S and 23S rRNA as well as the tRNAs from the *E.coli* R_2 state; all of these were rigid and fixed to ground. Corresponding residues on 23S and 16S rRNA were then pulled together, causing flexible alignment of these two subunits.

3.2. *Fitting atomic resolution structures to the electron density resulting from cryo-EM reconstructions of R_F*

R_F continues to be the subject of intense structural and dynamic research. This has been primarily driven by: (i) the availability of atomic resolutions structures of R_1; (ii) the possibility that, like R_1, R_F is a potential target for novel antibiotics; and (iii) the realization that a structural and dynamic understanding of R_F is necessary in order to fully understand the mechanism of the R_1 to R_F

transition. Despite the great importance of this state, however, atomic resolution structures have not yet been fitted into the electron density map resulting from all or even the majority of cryo-EM reconstructions of this conformational state of the pre-translocation ribosomal complex. As a result, Molecular Dynamics studies that may assist structure-based drug design have no structural point from which to begin. Interpolated trajectories which could begin to elucidate the path of tRNA during the R_1 to R_F transition lack a crucial endpoint.

In published work, structural coordinates for Elongation Factor G, the hybrid P/E configured tRNA, and a small number of additional components were fitted to a electron density map of the *T. thermophilus* R_F (EMD-1315)[2]. In this work, we add the 16S, 23S, and 5S rRNAs and most of the r-proteins.

Our main task was to fit an existing all-atom *probe* to a *target* electron density map. The most general methods available allow all bonds in the probe to vary in length, angle, and dihedral during the course of the fitting. One such method is Molecular Dynamics Flexible Fitting [11, 12]. However such methods are expensive, typically requiring parallel computers and significant run time. A popular alternative approach consists of three steps as follows:

1) Begin with rigid-body fitting, under which the probe has *no* flexibility, and the entire molecule is fitted to the electron density of the target using only rigid body rotations and translations.
2) If the molecule exhibits domain motions much of the flexibility can be recovered by breaking up the model into multiple fragments and adjusting each fragment separately into the electron density map. The natural boundaries between such rigid fragments are the hinge points connecting rigid domains; multiple experiments and calculations have been done to locate these hinges in the ribosome as we will explain below.
3) As a final step, anneal the gaps between fitted fragments belonging to a single RNA or protein chain; we will describe how the last structure of the R_2 to R_F motion provides this.

For step 1, we used SITUS COLORES to do the initial rigid body fitting of the entire ribosome[13, 14]. The next step, in which the probe is divided into fragments for adjustment into the map, requires a selection of hinge points. Fortunately this topic has been well studied. The rRNA-based neck domain of the small ribosomal subunit, which connects the head to the body/platform domains of the small ribosomal subunit, has long been known to be flexible[8]. Likewise, Noller and coworkers have found that by Translation-Libration-Screw Motion Determination (TLSMD) that the beak domain of the small ribosomal subunit and the L1 stalk domain of the large ribosomal subunit have the highest displacements about their librational axes[15], indicating a hinge point at the base of each of these two domains. Thus we divided the *probe* into six rigid pieces corresponding to the body, head, and beak domains of the small ribosomal subunit (along with their attendant proteins), the L1 stalk domain of the large ribosomal subunit (along with r-protein L1), the remainder of the large ribosomal subunit, and the tRNA. Since the probe has already been rigidly fitted at this point, the fragments created as described are already close to their correct positions in the electron density map. Thus an exhaustive search is not required, only a local adjustment. For this, Chimera's[16] *Fit in Map* feature is useful.

In the last step of the fitting, we correct the unnatural bond geometries spanning the gaps between fragments. This is done by taking the last structure resulting from the R_2 to R_F motion, which conserved bond lengths and angles throughout.

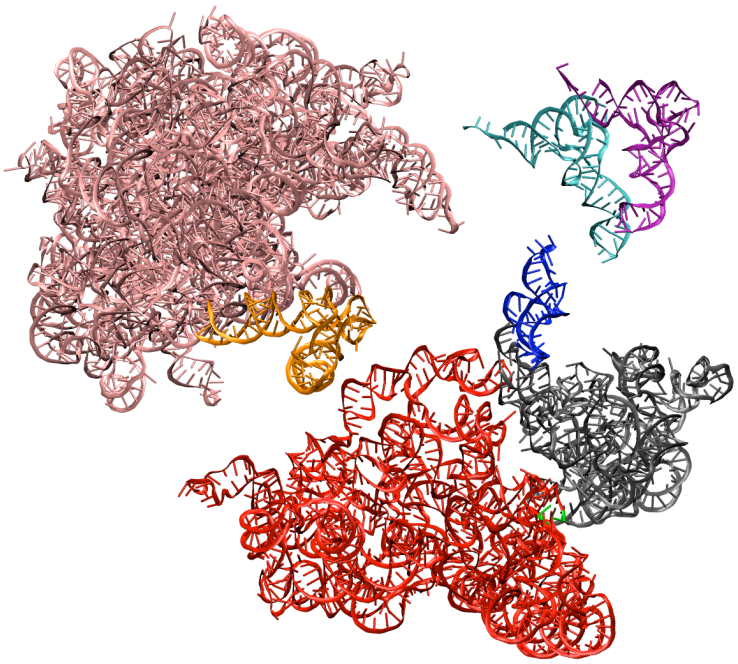

Figure 1. Choice of rigid domains for Cryo-EM fitting and creating *T.thermophilus* R2 structure (exploded view)

For fitting to Cryo-EM density: Following theoretical and experimental results described in the text, we broke up 16S into body (red), head (grey), and beak (blue). The "neck" connecting the head and body is shown in green for reference. The L1 stalk (orange) was separated from the rest of 23S (pink). The two tRNAs (cyan and purple) were independent bodies. Proteins (not shown) were attached rigidly to the corresponding 23S or 16S domain. The subunits were otherwise free to translate and rotate. For creating *T.thermophilus* R2 structure: The mentioned domains were left rigid as above, but instead of breaking 16S and 23S into fragments, we flexibilized hinge regions at the base of the L1 stalk, in the neck, and at the base of the beak.

3.3. *Generating the R_1-R_2-R_F trajectory*

In the last stage of our work we used a variation of our morphing technique to generate a controlled sequence of motions transforming the R_1 to R_2 to R_F state. We used the R_1, R_2 and R_F structures as fully-rigid, immobile templates much as before, but the aligned (or model) molecule was a ribosome which only one hinge – in the neck. The 23S was completely rigid and fixed to ground. tRNA was rigid (except for the 4 residues in the acceptor terminus) and could undergo rigid-body motion. 16S had a single flexible hinge in the neck region and could also undergo overall translation and rotation. 16S residue 1338 has been implicated in stabilizing the P/E site tRNA [10], therefore we connected this residue to tRNA residue 41 using a Sugar Edge / Sugar Edge interaction force, to approximately maintain an interaction observed in R_1, R_2, and R_F. We applied collision detecting spheres (to approximately represent steric repulsion) to the tRNA and to segments of 16S and 23S that might otherwise clash with tRNA (see Discussion).

We structurally aligned the ribosome model to R_1 to generate a starting point for our trajectory. We then aligned the model to R_2 and inspected the motion from R_1 to R_2. We then aligned the model to R_F. The trajectory of conformational change from R_1 to R_2 to R_F was the source of considerable insight as we will discuss.

Since it is not known whether full-length tRNAs in R_2 are in the classical or hybrid configuration, we generated an additional trajectory in which the tRNA remains in the classical state until 16S is fully rotated into the R_F conformation. The entire process is controlled with a single RNABuilder input file. The model is parametric in that global variables can be changed to easily generate any alternative ordering of these steps. Additional experimental information can be used to alter or constrain the motion, conversely the generated trajectory can help design focused experiments to generate further constraints.

4. Results

4.1. *Creating the T. thermophilus R_2 structure*

As mentioned a *T. thermophilus* ribosome in state R_1 was flexibly aligned to the *E.coli* ribosome in state R_2. We observed that as desired, proteins from R_1 were carried along with the RNA motion, and tRNAs moved in such a way as to maintain contact with their binding sites. The RMSD computed based on aligned glycosidic nitrogen atoms in 16S and 23S was initially 8.1Å and dropped to 2.9Å after 30 minutes of computer time. The degree of alignment can be qualitatively appreciated in (Figure 2). In a demonstration of convergence, we continued the calculation for an additional 127 minutes during which the RMSD remained nearly constant.

1.1. *Validation of the fitting of atomic resolution structures to the electron density from cryo-EM reconstructions of R_F*

In order to validate our fitting of atomic resolution structures into the electron density from cryo-EM reconstructions of R_F, we demonstrate that key molecular contacts expected or experimentally determined within R_F are recapitulated in our model. In particular, the detailed interactions of the tRNA aminoacyl-acceptor ends with the 23S rRNA within the peptidyl transferase center of the large ribosomal subunit are recovered (Figure 3).Also, the intersubunit bridges connecting the 23S rRNA with the body/platform of the 16S rRNA are recapitulated. Intersubunit bridge B4, which was predicted by Spahn (REF) and later Cate [17] to be maintained throughout the R_1 to R_F transition, indeed remains remains intact in our model (Figure 3).

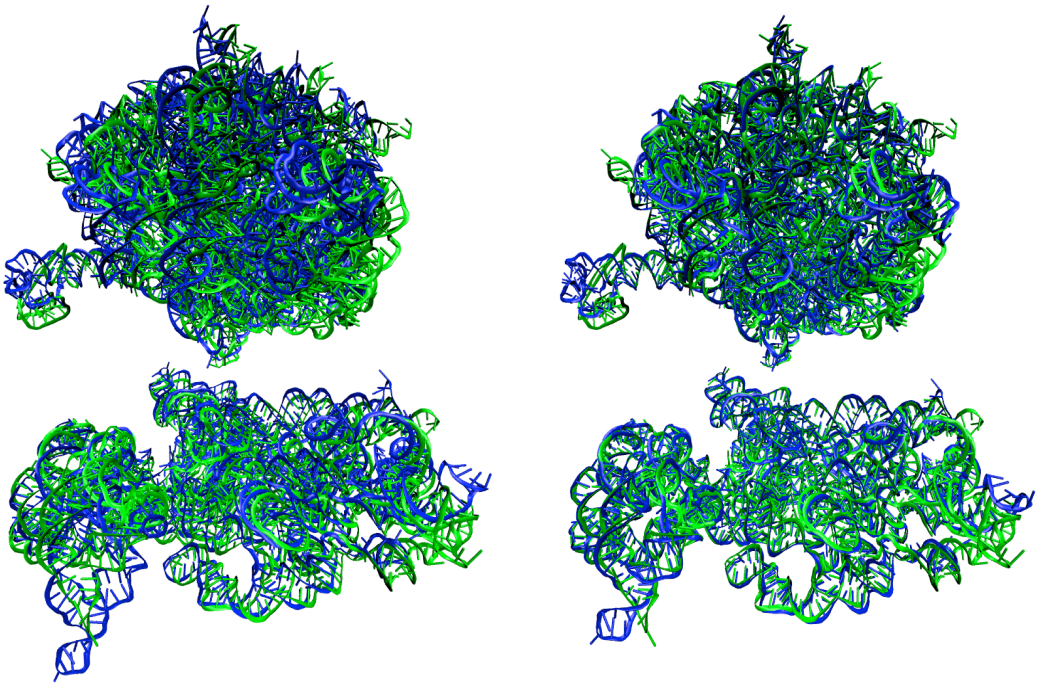

Figure 2. Morphing the *T.thermophilus* ribosome in state R1 onto the E.coli ribosome in state R2.

The *thermophilus* 23S (upper subunit) and 16S (lower subunit) are in blue. The E.coli 23S and 16S are in green. Additional *thermophilus* RNA and protein subunits are not shown. We included no E.coli subunits other than 23S and 16S. The thermophilus ribosome had hinges in the neck, base of the beak, and base of the L1 stalk. The E.coli ribosome was fully rigid and fixed to ground. tRNAs were attached to thermophilus P/P and E/E sites using base pairing and other forces and adjusted their positions as 16S and 23S moved. Thermophilus mRNA, 5S, and protein subunits were fully rigid and fixed to the corresponding 23S or 16S domain. Left panel: initial, rigid-body alignment. Note that blue and green are misaligned by as much as a helical diameter. Right panel: final alignment. Note that blue and green are now much more closely aligned. RMSD based on aligned glycosidic nitrogen atoms in 16S and 23S was initially 8.1Å (left) and converged to 2.9Å (right).

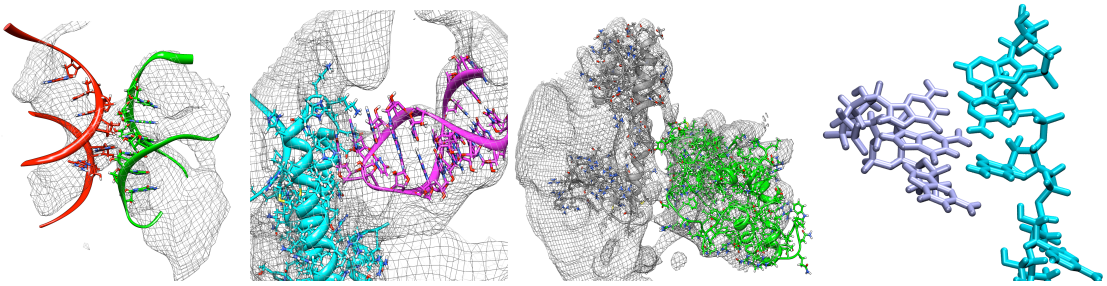

Figure 3. Intersubunit contacts.

The fitted RF model recapitulates bridge B3 (left panel). Bridge B4 was believed by earlier workers to remain in contact throughout ratcheting; the contact is maintained in our model (left-center panel). In bridge B1b/B1c (right-center panel), proteins S13 and L5 are connected by substantial regions of density, and the fitted proteins are in range to make contact. The A/P site tRNA acceptor (cyan, right panel) makes the correct base-pairing contacts with the 23S P site (purple).

4.2. *R1-R2-RF trajectory*

The trajectory of motion produced three main types of evidence which may be a source of insight. First, the residues to which we applied sterics (based on trial and error runs) may have functional importance. The aligned R_1, R_2 and R_F structures, even as static coordinates, may provide useful insight into the mechanism of motion. Our final trajectory as well as various alternative trial trajectories suggest constraints on the order and correlation of the motion of domains.

We applied sterics to H80/L80. Note that capital H indicates a helix in 23S, lowercase h indicates a 16S helix; similarly L/l indicates a loop and J/j indicates a junction in 23S/16S. Note also we are following Yusupov numbering for helices [18]. The H80 region contacted the acceptor terminus of the tRNA in some runs. In our model we left the acceptor terminus flexible so it simply sways out of the way. We also applied steric spheres to H69. When no sterics were applied here, the tRNA dropped down in some runs as the body moved away from 23S during 16S subunit rotation (Figure 4). We also applied sterics to the "gate" in 16S (h24, j29-42), beyond which the tRNA ASL should not pass (Figure 3). These and more possible interactions are listed in Table 1.

Subunit	**Residues (our num.)**	**Residues (consensus numbering)**	**Region**	**Notes**
tRNA	10-20	6-16	Inside elbow	Contacts H80/L80
	30-50	26-46	Anticodon stem-loop	Contacts 16S (gate and surroundings)
	74-80	70-76	Acceptor terminus	Contacts 23S (various points)
23S	1829-1847	1907-1925	H69	Contacts tRNA inside elbow
	1781-1785	1850-1854	H68 (int. loop)	
	2135-2142	2252-2259	H80	Contacts tRNA acceptor terminus
	2316-2321	2433-2438	H74	
16S	676-679	693-696	h23	
	771-775	788-792	h24	Part of gate
	1208-1212	1227-1231	h30	
	1318-1322	1337-1341	j29-42	Part of gate
	1474-1475	1497-1498	h44	

Table 1 : Residues needing collision-detecting spheres to prevent steric clashes.

We used preliminary runs to determine which 16S and 23S residues tRNA would contact in its trajectory from P/P to P/E sites. We applied steric spheres to the interacting residues. The contact points are suggested for experimental validation.

We aligned the R_1 and R_2 crystallographic structures and our fitted R_F structure to each other based on 23S rRNA. We observed that all three have tRNA anticodons very near to each other (Figure 5). For this reason it was quite easy for us to generate a classical-state R_2 model without prohibitive steric clashes, while Jamie Cate's R_2 model is in the hybrid state. The classical-state R_2 structure, however, did not have the tRNA contact with 16S residue 1338, as we will discuss, whereas all three experimental structures exhibit the residue-1338 contact.

We generated R_1-R_2-R_F trajectories ordering the motion in various ways. We tried moving the head, body, and tRNA separately; while this was sterically possible, the residue-1338 contact had to be broken to do it. By moving the head and body from R_1 to R_2 without moving the tRNA, we

generated a classical-state R_2 conformation, which of course did not have the 1338 contact. We found the results more credible when the head, body, and tRNA were moved at the same time, particularly since we were able to approximately maintain the contact using the base-pairing force mentioned between 1338 and residue 41. The reported final trajectory therefore has all three units moving together.

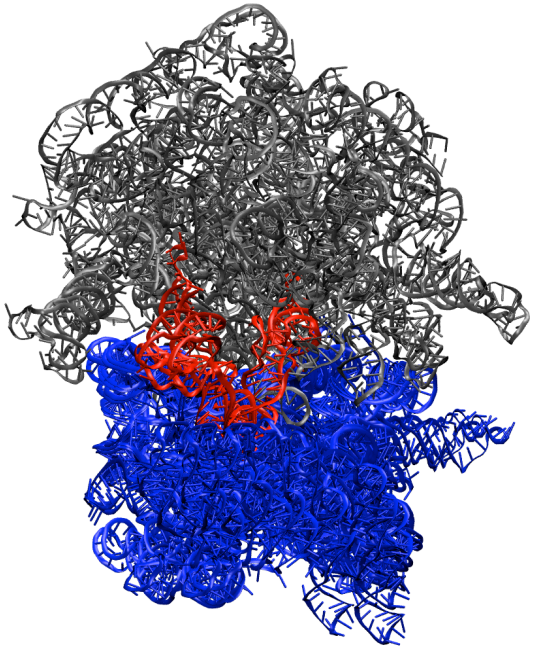

Figure 4. Putative motion from R1 to R2 to RF, with 23S fixed in space.

Composite view of the three main stages of the conformational rearrangement. The rightmost of the (red) tRNAs corresponds to the classical-state *T.thermophilus* R_1 structure (Protein Data Bank ID: 2J02 and 2J03), followed by the hybrid-state tRNA fitted by Jamie Cate to the R_2 structure (solved crystallographically in *E.Coli,* PDB ID: 3I1M & 3I1N, here modeled in *T.Thermophilus*). The leftmost tRNA was fitted by us to the CryoEM density map of the hybrid-state R_F structure (EMBL 3D-EM database ID EMD-1315). All three 16S conformations are shown superimposed (blue). The 23S subunit (grey) is kept rigid and stationary throughout. Note that the three anticodon stem-loops of the tRNAs are in nearly the same position throughout the motion, relative to 23S.

5. Discussion

In this work we modeled the trajectory of conformational change as the ribosome moves from the classical to the hybrid state, with an emphasis on the tRNA which moved from the classical P/P to the hybrid P/E configuration. Toward this end, we created a *T. thermophilus* ribosome in the R_2 state, as well as an all-atom fitted model of the ribosome in the R_F state; these are provided as supplementary materials and may be useful for further studies. The trajectory from R_1 to R_2 to R_F provides insight and suggests further experiments from three perspectives: the steric contacts, the aligned static structures, and the interpolated structures.

The regions where it was necessary to apply steric spheres are suggestive of specific experiments. In any of the contacting regions, one can imagine generating mutant ribosomes in which the steric barrier is either increased or eliminated. For instance: the part of the gate on the head domain is clearly important, since it includes residue 1338. What would happen if we eliminated the part that is on the body domain? We also noticed that H69 prevents the tRNA from moving down towards the mRNA. What would happen if it, too, disappeared? What about H80, which the acceptor terminus must brush past? What if the barrier were even higher? And residue 1338—is it really always in contact with tRNA? Could this be probed with a combination of mutagenesis and single-molecule fluorescence resonance energy transfer (smFRET) experiments?

Some interesting insight comes just from the static R_1, R_2, and R_F structures. First, after fitting all-atom subunit structures to the density map of R_F, we realized that the crucial 1338-41 contact is maintained in this state as well, thus validating the prediction of [10]. This was a key piece of evidence which encouraged us to enforce this contact throughout the motion. Second, aligning R_1,

R_2, and R_F structures based on 23S yielded an interesting finding—the P-site anticodons of the three structures are just a few angstroms apart. Thus the 16S P-site moves little with respect to 23S rRNA during the intersubunit rotation. This makes it quite easy to generate a clash-free model of R_2 with a tRNA in the classical P/P configuration. However, we believe that it is more likely for the tRNA to occupy the hybrid P/E configuration on the basis that this will maintain the 1338-41 base contact which is so clearly present in all three experimental static structures.

The trajectory itself is suggestive. First, maintaining the 1338-41 contact as we did implies a coordinated motion of the head and the tRNA. Since the anticodon does not move much, the motion is mostly a long translation of the aminoacyl acceptor end of the tRNA. Using this trajectory a donor/acceptor flurophore pair for smFRET experiments can be designed with one fluorophore attached to the tRNA and another to the head; we would predict that such a construct would exhibit a constant, static FRET value that is maintained throughout the R_1 to R_F transition. Second, we did not directly address the twisting motion of the neck, but the trajectory can be used to optimally place donor/acceptor fluorophore pairs spanning the head and body. Lastly, one can design a donor/acceptor fluorophore pair in order to determine how much time the ribosome spends in state R_2—perhaps with a donor/acceptor fluorophore pair spanning 23S rRNA and the body domain.

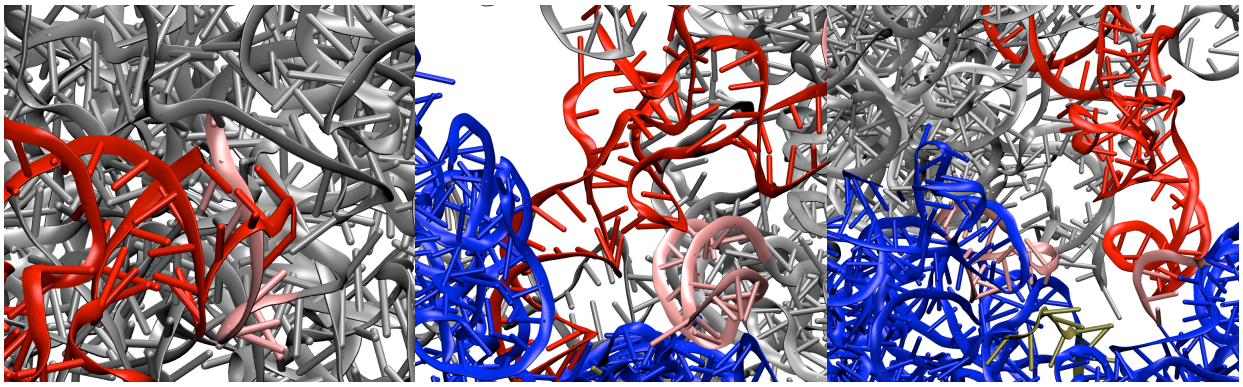

Figure 5. tRNA steric barriers.

Left panel: The acceptor terminus of tRNA (red) makes contact with H80/L80 (pink) of the 23S (grey). In nature tRNA may rotate, move away from 23S, or the floppy acceptor end may simply move out of the way. Middle panel: Contact between tRNA and H69 (pink) of 23S. In our model this forces tRNA to translocate laterally whereas without it tRNA might drop downwards to maintain contact with mRNA after body rocking. Right panel: Contact of the anticodon stem-loop with P-site barriers formed by h24 (pink) and the "gate" loop (residues 1335-1339) (also pink) in 16S (blue). tRNA cannot move fully into the P/E configuration until body and head have rotated.

Acknowledgements and availability

We thank Ruben Gonzalez for numerous discussions, guidance, and contributions to the text. We also thank Tom Cech and Martin Laurberg for illuminating discussions. Lastly, we thank Jamie Cate and Sean Connell for providing advice and unpublished structural coordinates. We provide starting coordinates, RNABuilder input files, the all-atoms fitted RF structure, the *T.thermophilus* R_2 structure, and the full trajectory for both R_1- R_2- R_F motions at https://simtk.org/home/ribosome-paper. RNABuilder can be downloaded at http://simtk.org/home/rnatoolbox.

References

1. Berk V, Cate JH: **Insights into protein biosynthesis from structures of bacterial ribosomes**. *Current opinion in structural biology* 2007, **17**(3):302-309.
2. Connell SR, Takemoto C, Wilson DN, Wang H, Murayama K, Terada T, Shirouzu M, Rost M, Schuler M, Giesebrecht J *et al*: **Structural basis for interaction of the ribosome with the switch regions of GTP-bound elongation factors**. *Molecular cell* 2007, **25**(5):751-764.
3. Ayton GS, Noid WG, Voth GA: **Multiscale modeling of biomolecular systems: in serial and in parallel**. *Current opinion in structural biology* 2007, **17**(2):192-198.
4. Glotzer SC PW: **Molecular and mesoscale simulation methods for polymer materials**. *Annu Rev Mater Res* 2002, **32**:401-436.
5. Flores S, Sherman, M, Bruns, C, Eastman, P, Altman, RB: **Fast flexible modeling of macromolecular structure using internal coordinates**. *IEEE Transactions in Computational Biology and Bioinformatics, submitted* 2010.
6. Flores S, Altman, RB: **Turning limited experimental information into 3D models of RNA** *RNA, submitted* 2010.
7. Flores S, Wan, Y, Russell, R, Altman, RB: **Predicting RNA structure by multiple template homology modeling**. *Proceedings of the Pacific Symposium on Biocomputing* 2010:216-227.
8. Zhang W, Dunkle JA, Cate JH: **Structures of the ribosome in intermediate states of ratcheting**. *Science (New York, NY* 2009, **325**(5943):1014-1017.
9. Selmer M, Dunham CM, Murphy FVt, Weixlbaumer A, Petry S, Kelley AC, Weir JR, Ramakrishnan V: **Structure of the 70S ribosome complexed with mRNA and tRNA**. *Science (New York, NY* 2006, **313**(5795):1935-1942.
10. Shoji S, Abdi NM, Bundschuh R, Fredrick K: **Contribution of ribosomal residues to P-site tRNA binding**. *Nucleic acids research* 2009, **37**(12):4033-4042.
11. Trabuco LG, Villa E, Mitra K, Frank J, Schulten K: **Flexible fitting of atomic structures into electron microscopy maps using molecular dynamics**. *Structure* 2008, **16**(5):673-683.
12. Birmanns WWaS: **Using Situs for Flexible and Rigid-Body Fitting of Multiresolution Single-Molecule Data**. *Journal of Structural Biology* 2001, **133**:193–202.
13. Chacon P, Wriggers W: **Multi-resolution contour-based fitting of macromolecular structures**. *Journal of molecular biology* 2002, **317**(3):375-384.
14. Fabiola F, Chapman MS: **Fitting of high-resolution structures into electron microscopy reconstruction images**. *Structure* 2005, **13**(3):389-400.
15. Korostelev A, Noller HF: **Analysis of structural dynamics in the ribosome by TLS crystallographic refinement**. *Journal of molecular biology* 2007, **373**(4):1058-1070.
16. Eric F. Pettersen TDG, Conrad C. Huang, Gregory S. Couch, Daniel M. Greenblatt, Elaine C. Meng, Thomas E. Ferrin: **UCSF Chimera—A Visualization System for Exploratory Research and Analysis**. *Journal of Computational Chemistry* 2004, **25**:1605–1612.
17. Schuwirth BS, Borovinskaya MA, Hau CW, Zhang W, Vila-Sanjurjo A, Holton JM, Cate JH: **Structures of the bacterial ribosome at 3.5 A resolution**. *Science (New York, NY* 2005, **310**(5749):827-834.
18. Yusupov MM, Yusupova GZ, Baucom A, Lieberman K, Earnest TN, Cate JH, Noller HF: **Crystal structure of the ribosome at 5.5 A resolution**. *Science (New York, NY* 2001, **292**(5518):883-896.